

# Dielectric properties of pyrolysed polyimide films

G. A. NIKLASSON, I. A. SERBINOV\*

*Physics Department, Chalmers University of Technology, S-412 96 Göteborg, Sweden*

We have studied the dielectric properties, in the frequency range  $10^{-4}$ – $10^7$  Hz, of polyimide films that were heat treated in vacuum in order to increase their conductivity. Films with electrical properties at the threshold between the insulating and conducting states show an anomalous low frequency dispersion composed of two power laws. The experimental results are consistent with electrical conduction in random one-dimensional chains. Also contact effects are present in our spectra. We conclude that the conducting inclusions formed upon heat treatment of polyimide films are arranged in linear chains.

## 1. Introduction

Polyimide [1, 2] is a high temperature stable polymer commercially available as Du Pont Kapton. It exhibits good electrical and mechanical properties as well as chemical resistance [1]. It is used as an electrically insulating film and as a protective coating. The thermal stability of polyimide upon heating in vacuum or in different atmospheres has attracted much attention, [3–5]. When heated in air the polymer volatilizes at temperatures in excess of 400°C [3, 4]. Upon heating in vacuum or an inert atmosphere, however, only ~40% volatilization takes place [3, 4], and the product of the pyrolysis is an electrically conducting carbonized film [3–5]. The electrical properties of the pyrolysed film have been the subject of intense study, [6–10]. Electrical conduction seems to be of the hopping [6] or tunnelling [7, 8] type, which suggests that the pyrolysed polyimide is a composite consisting of conducting regions in an insulating matrix. The nature of the conducting regions is not clear, though. They may consist of pure carbon [7, 8] or of a continuous network of aromatic rings [5, 9] obtained by a structural rearrangement during heating. Pyrolysed polyimide has been suggested as a gate material for transistors [11]. Photosensitive polyimide can also be used to produce circuitry on semiconductor substrates.

Recently we studied the kinetics of the transition from the insulating to the conducting state of polyimide heat treated in vacuum at different temperatures. We found [12] that the process follows a simple activated behaviour with an activation energy equal to the fundamental energy gap of polyimide. In this paper we study the a.c. dielectric properties of polyimide close to the transition. Dielectric spectroscopy can give information on the electrical conduction mechanisms as well as the structural arrangement of the units partaking in the conduction process. Our results show that the conducting regions seem to be arranged in chains.

In Section 2 we describe the experimental procedures

applied by us. Section 3 reports on the results of the dielectric measurements and recapitulates the most important results on the kinetics of the insulator-conductor transition. We interpret our data in Section 4 where we also briefly review some basic theory of the dielectric response based on the random walk concept.

## 2. Experiment

In our studies we used Kapton foils of thickness 50  $\mu\text{m}$  obtained from the producer. The films were heat treated at different temperatures for different times in a vacuum chamber kept at a pressure of ~0.1 torr. During heat treatments at temperatures above 250°C the samples become progressively darker indicating that conversion to a carbon-rich phase has started in certain regions. The darkening of the samples precedes the occurrence of measurable electrical conduction. In order to obtain samples with conductivities in the transition region between the insulating and conducting states, we had to use temperatures between 400 and 450°C and times in excess of one hour. After heat treatments contacts of silver paint were applied on the upper and lower sides of the films. For electrical measurements the upper side was contacted by pressing a spring-loaded needle against it, while the bottom contact was pressed against a metal plate.

Dielectric measurements at frequencies in the range  $10^{-4}$  Hz–4 kHz were performed by the computerized system sketched schematically in Fig. 1. The sample was contacted on a stage in a shielded container and a sine wave was applied between the contacts by a HP3325 A function generator. The current flowing through the samples was amplified by a Keithley 427 current amplifier. The signal from the current amplifier as well as that from the function generator was converted to digital form and stored in a computer. From the amplitudes and the phase difference between the signals the complex dielectric permittivity,  $\epsilon(\omega) = \epsilon_1(\omega) + i\epsilon_2(\omega)$  was easily obtained. The computer

\* Permanent address: Institute of Radio Engineering and Electronics, Academy of Sciences, Marx Avenue 18, Moscow, USSR.

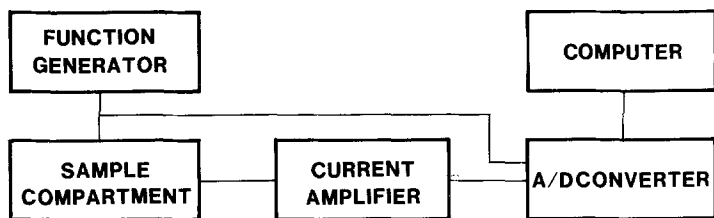


Figure 1 Schematic diagram of system for the measurement of dielectric properties in the frequency range  $10^{-4}$ – $4 \times 10^3$  Hz.

also corrects the values for the phase lag introduced by the finite rise time of the current amplifier. The maximum frequency that can be used for measurements in this system is about 4 kHz and is set by the speed of the amplifier.

For measurements at frequencies in the range  $10^4$ – $10^7$  Hz we used a conventional capacitance bridge. Contact areas were measured by an optical microscope. The thickness of the films was taken to be  $50 \mu\text{m}$  as specified by the manufacturer, although a shrinkage of the film during pyrolysis cannot be ruled out. This possibly gives an uncertainty in the absolute values of  $\epsilon(\omega)$ . However, it does not affect our arguments, since the form of the curve is not affected by such an effect.

### 3. Results

In our earlier study [12] we found that the pyrolysis of polyimide upon heating in vacuum can be described by the Arrhenius equation

$$\tau = t_0 \exp(\Delta E/kT), \quad (1)$$

where  $\tau$  is a delay time corresponding to the time it takes for the polyimide foil to go over to the pyrolysed state,  $t_0 \sim 10^{-13}$  sec is a typical reciprocal phonon frequency,  $\Delta E$  is the activation energy,  $k$  is Boltzmann's constant and  $T$  is the temperature. The increase in optical density upon heating of polyimide [12] can be fitted to Equation 1 with  $\Delta E \sim 2.0$  eV, which is close to the value of the fundamental energy gap of the material.

The transition from the insulating to the conducting state is slower than the optical transition. In Fig. 2 we plot the electrical conductivity as a function of  $kT \ln(t/t_0)$  for our films. Here  $t$  denotes the heating time. In the figure we have also included some literature data for films heat treated in vacuum [3, 4] and in a nitrogen atmosphere, [6, 10]. It is seen that the transition takes place at  $\sim 2.3$  eV for films heated in vacuum and at  $\sim 2.6$  eV for films heated in nitrogen. The shape of the conductivity curve close to the transition is presently not understood. It is to be noted that electrical conductivity is not proportional to the concentration of conducting material. The sharp rise of conductivity takes place at a certain critical concentration, the percolation threshold, which may vary depending on experimental conditions. On the other hand the optical density of a film is to a first approximation proportional to the concentration of absorbing material. Therefore we think that the optical measurements gives a better value of  $\Delta E$  than the electrical measurements.

Dielectric measurements on as received polyimide films showed an essentially frequency independent dielectric function with  $\epsilon_1 \sim 3.3$ – $3.6$  and a loss tangent  $\epsilon_2/\epsilon_1 \sim 2$ – $4 \times 10^{-3}$ . These values are consistent

with literature data [13–16]. In polyimide strong loss peaks occur only at temperatures in excess of  $100^\circ\text{C}$  [13–15]. We observed that the loss tangent seemed to decrease somewhat upon low temperature annealing ( $kT \ln t/t_0 < 2.15$  eV). Such an effect has been observed before [16] and may be due to either loss of adsorbed water or paracrystalline ordering [17] of the material.

We now turn to the description of the dielectric properties of samples close to the insulator–conductor transition. Spectra over the whole  $10^{-4}$  Hz–4 MHz range are given for two of our samples in Fig. 3. The sample in Fig. 3a, which was heated at  $395^\circ\text{C}$  for 5 h, is representative of the early part of the transition. At high frequencies the almost flat  $\epsilon_1(\omega)$  and  $\epsilon_2(\omega)$  curves representative of the insulating phase can be seen. The dielectric loss  $\epsilon_2(\omega)$  is much higher than for unaged films, however. The influence of the conducting phase is seen in the dispersion of  $\epsilon_1(\omega)$  and  $\epsilon_2(\omega)$  at frequencies below 10 kHz. Apart from a very slight bump around 0.1 Hz the curves follow a so-called anomalous low-frequency dispersion [18–20] (ALFD)

$$\epsilon_1(\omega) - \epsilon_\infty \sim \epsilon_2(\omega) \sim \omega^{-p}, \quad \omega < \omega_c \quad (2a)$$

$$\epsilon_1(\omega) - \epsilon_\infty \sim \epsilon_2(\omega) \sim \omega^{n-1}, \quad \omega > \omega_c \quad (2b)$$

where  $\epsilon_\infty$  is the high frequency dielectric constant and the exponents  $p$  and  $n$  can have values between zero and unity. Such behaviour is often seen in systems having charge carriers of low mobility [18]. A notable feature of this dielectric response (and of the curve in Fig. 3a) is that no d.c. conductivity is observed even at the lowest frequencies that have been measured.

In Fig. 3b the dielectric response of a sample heated at  $455^\circ\text{C}$  for one hour is shown. There are several similarities with the behaviour of the sample in Fig. 3a. At high frequencies the power law of Equation 2b can be seen. Between 10 and 1000 Hz a step in  $\epsilon_1(\omega)$  and a slight bump in  $\epsilon_2(\omega)$  are apparent. This is probably due to a relaxation process superimposed on the underlying ALFD. We believe that these features correspond to the almost invisible bumps around 0.1 Hz in Fig. 3a and return to the interpretation of this structure later. At still lower frequencies  $\epsilon_2(\omega)$  satisfies Equation 2a with  $p$  equal to or very close to unity, while  $\epsilon_1(\omega)$  is fairly constant. If  $\epsilon_1(\omega)$  really becomes constant at low frequencies then we have an ordinary d.c. conductivity, which is given by the equations [20]

$$\epsilon_1(\omega) = \epsilon_0 \quad (3a)$$

$$\epsilon_2(\omega) = \sigma/\omega \quad (3b)$$

where  $\epsilon_0$  is the static dielectric constant and  $\sigma$  is the d.c. conductivity. However, we could not measure  $\epsilon_1(\omega)$  below  $10^{-2}$  Hz because of the limited accuracy in the determination of the very small phase differences involved. The slight increase in  $\epsilon_1(\omega)$  near  $10^{-2}$  Hz

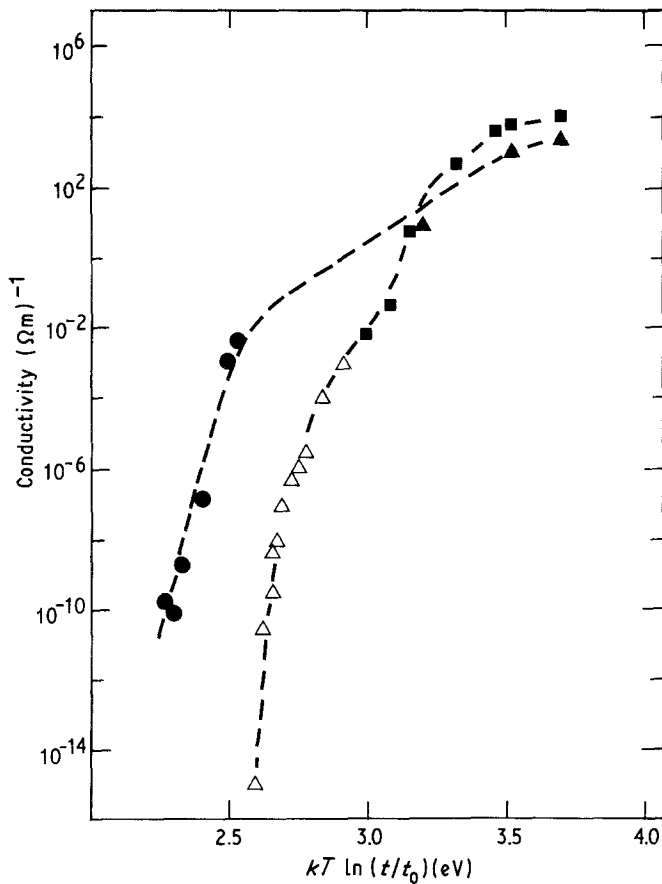


Figure 2 Electrical conductivity as a function of the energy parameter  $kT \ln(t/t_0)$  for polyimide films pyrolysed at temperature  $T$  for the time  $t$ . Results are for films heat treated in vacuum: ● This work, ▲ [3] and for films heat treated in nitrogen: □ [6], △ [10].

may indicate that the ALFD of Equation 2a with  $p$  very close to unity is present rather than a d.c. conductivity. The primary effect of the higher conductivity of the sample in Fig. 3b as compared to that in Fig. 3a is to shift the structures in the curve to higher frequencies. This is even more apparent if samples with still higher conductivity are studied. For samples with conductivities in the range

$10^{-3}$ – $10^{-2}$  ( $\Omega\text{m}$ ) $^{-1}$  the d.c. conductivity is seen over almost the whole of our observable frequency range.

We now describe the determination of the power law exponents  $p$  and  $n$  in Equation 2. They can be obtained by fitting straight lines to the appropriate portions of log-log plots of the dielectric response such as Fig. 3. As an additional check one can also use

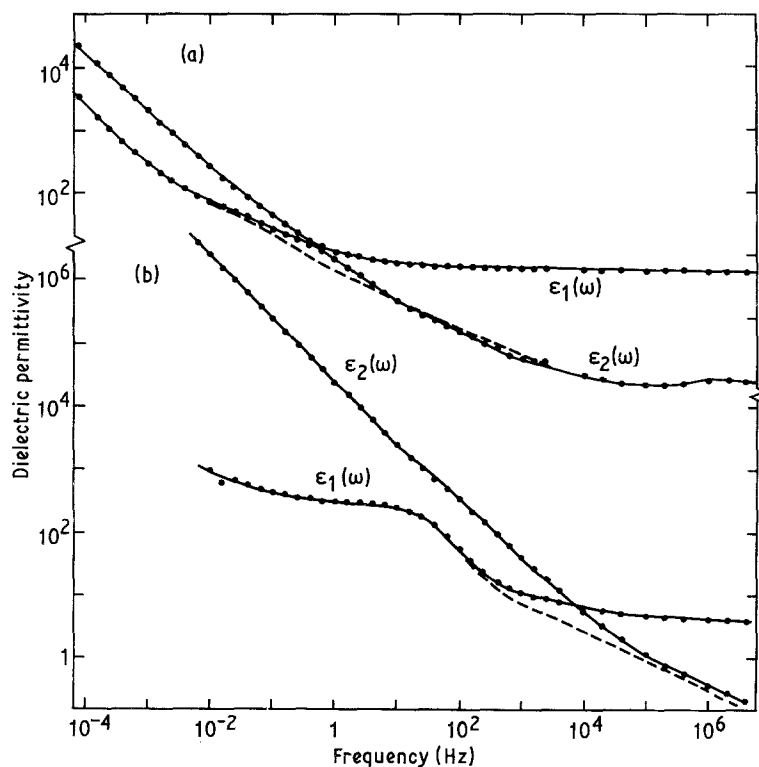


Figure 3 Real and imaginary parts of the dielectric permittivity for two of our pyrolysed polyimide films are shown as a function of frequency. Points denote experimental data and the lines are drawn as a guide for the eye only. Broken lines denote the function  $\epsilon_1(\omega) - \epsilon_\infty$ . The films were heat treated at a pressure of 0.1 torr for (a) 5 h at 395°C and (b) 1 h at 455°C. Values of  $kT \ln(t/t_0)$  were (a) 2.29 eV and (b) 2.39 eV.

TABLE I Values of exponents  $p$  and  $n$ , the crossover frequency  $\omega_c$  and the quantity  $kT \ln(t/t_0)$  for pyrolysed polyimide films

Sample	$kT \ln(t/t_0)$ (eV)	$\omega_c$ (Hz)	$n$	$p$
1	2.28	1	0.50	0.95
2	2.29	0.4	0.53	0.90
3	2.33	40	0.49	1
4	2.39	$5 \times 10^3$	0.49	1
5	2.49	$> 10^7$	-	1

the relations [20]

$$(\varepsilon_1(\omega) - \varepsilon_\infty)/\varepsilon_2(\omega) = \tan(n\pi/2), \quad \omega > \omega_c \quad (4a)$$

$$(\varepsilon_1(\omega) - \varepsilon_\infty)/\varepsilon_2(\omega) = \tan((1-p)\pi/2), \quad \omega < \omega_c \quad (4b)$$

This method is best at low frequencies where the exact numerical value of  $\varepsilon_\infty$  is not so important, since it is much less than  $\varepsilon_1$ . We have analysed the ALFD of our samples by these methods. The results are given in Table I. It is seen that the values of  $p$  are in the range 0.90–0.95 for the least conducting samples, and then rapidly approaches one as the samples become more conducting. The values of  $n$  are more uncertain as the power law of Equation 2b in some of the samples is visible only over a limited frequency range. However, all of our data are consistent with the value  $n = 0.5$  with an estimated maximum uncertainty of  $\pm 0.05$ .

Now we wish to interpret the dielectric spectrum in terms of the structural arrangement of the conducting inclusions. To this end we model the conductivity as being due to a random-walk process. We will also argue that the relaxation process that is superimposed on the ALFD is due to contact effects.

#### 4. Theory and discussion

The pyrolysed polyimide is probably a quite disordered material containing conducting regions in an insulating matrix. We assume that charge transport proceeds between localized states or conducting particles in the material. The transport mechanism may be hopping or tunnelling. In addition trapping may be of some importance. The constitutive relation at a point in the material between the time-dependent current  $J(t)$ , the electric field  $E(t)$  and the charge carrier density  $n(t)$  can be written as [21, 22]

$$\begin{aligned} \bar{J}(t) = & -\nabla \int_{-\infty}^t D(t-t') n(t') dt' \\ & + \frac{e}{kT} \int_{-\infty}^t D(t-t') n(t') \bar{E}(t') dt' \end{aligned} \quad (5)$$

where  $e$  is the electron charge and  $D(t)$  is a generalized diffusion coefficient. The first term is due to diffusion of charge carriers and the second is the drift term due to the applied electric field. The generalized diffusion equation (5) can be obtained from the generalized Master equation describing the microscopic conduction process, [21–23]. We now apply this treatment to the case when the charge carrier transport is described by a random walk. The Fourier transform of the mean square displacement of the walker,  $\langle r^2(t) \rangle$  is related to

the complex diffusion coefficient by [24]

$$D(\omega) = -\frac{1}{6} \omega^2 \int_0^\infty dt e^{-i\omega t} \langle r^2(t) \rangle \quad (6)$$

The dielectric permittivity is immediately obtained as [24, 25]

$$\varepsilon(\omega) = in_0 e^2 D(\omega)/k_B T \omega, \quad (7)$$

where  $n_0$  is the average density of charge carriers.

Recently, a scaling approach has been suggested [25, 26] which makes it possible to relate the dielectric permittivity to the probability for a charge carrier, that was at the origin at time zero, to return there at time  $t$ ,  $P_0(t)$ . The result [25, 26]

$$\langle r^2(t) \rangle \sim (P_0(t))^{-2/D} \quad (8)$$

where  $D$  is the dimensionality, should be applicable to diffusion both on regular and fractal [27–31] lattices.

We next consider the dielectric properties of chain structures which should be important in polymeric samples. In a linear chain we have one-dimensional diffusion with  $P_0(t) \sim t^{-1/2}$ . For a regular chain this leads directly to a constant  $\sigma(\omega)$ , i.e. we have a pure d.c. conductivity, [25]. However the states in a chain may be clustered on short length scales. In that case the d.c. conductivity level is set by the most difficult transitions. At short length scales or high frequencies the transitions are easier and the conductivity becomes higher.

The high frequency behaviour may be obtained as a limiting case of conduction on a fractal structure, for which we obtain [32]

$$\varepsilon(\omega) \sim \omega^{-D_f/D_w}, \quad (9)$$

where  $D_f$  is the fractal dimension and  $D_w$  is the random walk dimension. Equation 9 is applicable for frequencies larger than a crossover frequency  $\omega_c$ . For a linear chain  $D_f = 1$  and  $D_w = 2$ , which would yield the behaviour

$$\varepsilon(\omega) \sim \omega^{-0.5} \quad \omega > \omega_c \quad (10a)$$

$$\varepsilon_1(\omega) = \varepsilon_0 \quad \varepsilon_2(\omega) \sim \omega^{-1} \quad \omega < \omega_c \quad (10b)$$

This is very close to the experimental results that we obtained for pyrolysed polyimide.

Above we interpreted the exponent  $-0.5$  at  $\omega > \omega_c$  as being due to a random walk of independent charge carriers on a linear chain. An alternative explanation can be given in terms of a cooperative effect involving many charge carriers. Actually this behaviour occurs in standard diffusion processes [20]. We have not been able to discriminate between these two possible explanations for the high frequency response.

For  $\omega < \omega_c$  we observed departures from pure d.c. behaviour for some of our films. In order to explain this we have to consider fractal time processes, which are expected to arise in disordered structures, for example in chains with configurational disorder. This kind of process can be modelled as a random walk where the charge carriers pause for a certain time before each step. The waiting-time distribution,  $\psi(t)$ , at long times becomes [33]

$$\psi(t) \sim t^{-1-D_f} \quad (11)$$

where  $D_f$  is the fractal dimension of the time process.

Equivalently we could have specified a distribution of transfer rates as done by Alexander *et al* [25]. This kind of distribution can be due to hopping between randomly distributed sites on a linear chain, to hopping with an exponential distribution of activation energies or to trapping in an exponential distribution of trapping states. The dimension  $D_1$  can be expressed in terms of microscopic hopping or trapping parameters [25]. Alexander *et al* [25] have solved this problem for a one-dimensional chain and obtained the asymptotic behaviour of  $P_0(t)$  and the conductivity at long times. The result is [25]

$$\varepsilon(\omega) \sim \omega^{-2D_1/(1+D_1)} \quad (12)$$

We think that the most probable interpretation of the dielectric response of the pyrolysed polyimide foils is in terms of a fractal time process on a structure consisting of linear chains. At  $\omega < \omega_c$  the fractal time process dominates the response. It is probably due to a random distribution of the carbonized inclusions in the chains, although trapping effects cannot be ruled out. At  $\omega > \omega_c$  on the other hand the chain structure is of prime importance. The dispersion of the dielectric permittivity is due to random walks or diffusion on the chains. The fractal time process is expected to give only minor modifications to  $\varepsilon(\omega)$  in the high frequency regime. We have thus arrived at a consistent picture of the dielectric response of pyrolysed polyimide, where the unifying element is the underlying chain structure of the polymer.

After having interpreted the ALFD behaviour of the pyrolysed polyimide films we must also explain the relaxation process which is seen most clearly as a step in  $\varepsilon_1(\omega)$  in Fig. 3b. The relaxation peak in  $\varepsilon_2(\omega)$  that is expected to accompany this structure is almost invisible due to the overlap with the strong ALFD dispersion. Relaxation peaks may originate from motion of charge carriers on finite clusters of conducting states that are separated from the main conduction channels. An alternative explanation is in terms of barrier layers at the contacts. We will argue that this latter effect is present in our samples. Consider the circuit model of Fig. 4a. A barrier region near the contacts is modelled by a capacitance,  $C$ . We model the bulk of the sample with a “universal” capacitor [20] of the form

$$\bar{C} = A(i\omega)^{n-1}. \quad (13)$$

So far we have not taken into account the near d.c. part of the dispersion that becomes dominant below  $\omega_c$ . This can be accounted for by a parallel resistance,  $R$ . The circuit in Fig. 4a is easily analysed; for the case when  $\bar{C} \ll C$  and  $R$  is relatively large we obtain the schematic behaviour depicted in Fig. 4b. If  $R$  is made smaller the d.c. contribution to  $\varepsilon_2(\omega)$  will become larger so that it overlaps with the relaxation peak. In our samples the d.c. part is so large that the relaxation peak almost cannot be seen at all. However it can be inferred from the step in  $\varepsilon_1(\omega)$  seen in Fig. 3b between 10 and 1000 Hz. The slope of this step is close to one for our samples which is in good agreement with the theoretical prediction  $2n - 2$  in Fig. 4b, if  $n = 0.5$ . Thus we have shown that the dispersion of the dielec-

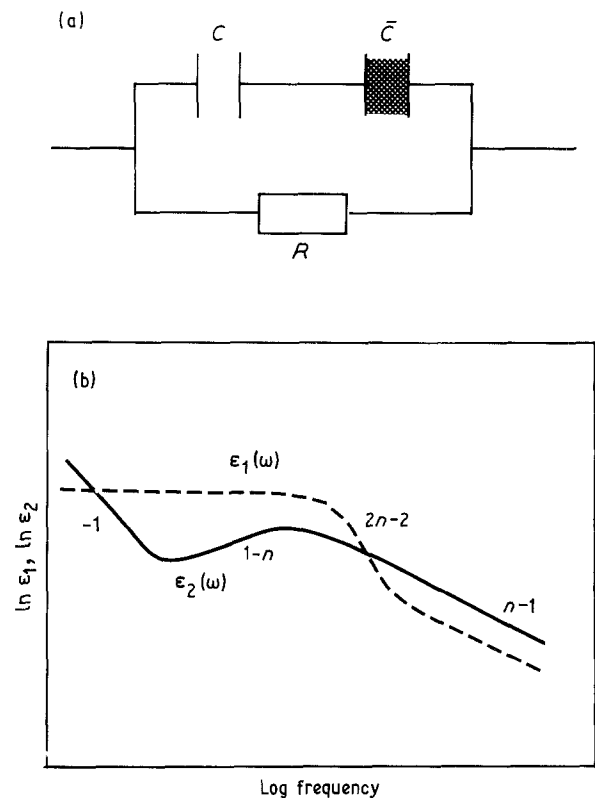


Figure 4 (a) Circuit diagram for a pyrolysed polyimide film including a contact capacitance  $C$ . The d.c. process is represented by a parallel resistance  $R$ , while the dispersive element  $\bar{C}$  is given by  $A(i\omega)^{n-1}$ . (b) Schematic behaviour of the dielectric permittivity for the circuit diagram in (a).

tric permittivity in our polyimide samples with high conductivity can be explained by the circuit model in Fig. 4a. In the samples with lower conductivity, such as that in Fig. 3a, the barrier effect is almost invisible, but for a slight hump in  $\varepsilon_1(\omega)$  near 0.1 Hz. The nature of the contact barrier remains obscure, though. It is surprising that it does not seem to affect the d.c. or near d.c. conductivity at low frequencies.

## 5. Conclusion

We have pyrolysed polyimide by heat treatment at a pressure of 0.1 torr. The dielectric permittivity in the frequency range  $10^{-4}$ – $10^7$  Hz was studied for samples close to the insulator–conductor transition. The dielectric response shows an anomalous low frequency dispersion. In addition a relaxation process which we ascribe to contact effects is present. The ALFD consists of two power laws in frequency. The low frequency exponent  $p$  is very close to one, while the high frequency exponent  $1 - n$  is close to 0.5. This is just what is expected for hopping or tunnelling conduction on a linear chain. Slight departures from  $p = 1$  are ascribed to the random arrangement of conducting states in the chain, or to trapping effects.

During the pyrolysis part of the polyimide is carbonized and it is probably the carbonized regions that become conducting. Conduction then proceeds by a hopping or tunnelling process between the conducting regions. Our dielectric measurements show that the conducting regions are randomly distributed in chains and thus preserve the underlying chain structure of the polymer. The conducting regions seem to be clustered

at the short length scales as can be inferred from the high-frequency part of the ALFD.

Finally we remark that the emerging understanding of dielectric spectra in terms of the underlying geometrical arrangement of conducting states makes dielectric spectroscopy an important tool for the electrical characterization of thin films. In particular the effect of degradation processes on the structure of dielectric materials is becoming feasible to study from this point of view.

### Acknowledgements

This work was financially supported by grants from the Swedish Board of Technical Development, the Swedish Natural Science Research Council and from ASEA Research and Development, Västerås, Sweden. We are grateful to K. Brantervik and C. G. Granqvist for discussions and assistance.

### References

1. C. E. SROOG, *J. Polym. Sci. Macromol. Rev.* **11** (1976) 161.
2. L. E. AMBORSKI, *Ind. Eng. Chem.* **2** (1963) 189.
3. S. D. BRUCK, *Polymer* **5** (1964) 435.
4. *Idem, ibid.* **6** (1965) 49, 319.
5. S. D. BRUCK, *J. Polym. Sci. C* **17** (1967) 169.
6. H. B. BROM, Y. TOMKIEWICZ, A. AVIRAM, A. BROERS and B. SUNNERS, *Solid State Commun.* **35** (1980) 135.
7. J. I. GITTLEMAN and E. K. SICHEL, *J. Electron Mater.* **10** (1981) 327.
8. E. K. SICHEL and T. EMMA, *Solid State Commun.* **41** (1982) 747.
9. C. Z. HU and J. D. ANDRADE, *J. Appl. Polym. Sci.* **30** (1985) 4409.

10. S. SAITO, T. TSUTSUI, S. TOKITO, T. HARA and H-T. CHIU, *Polymer J.* **17** (1985) 209.
11. D. R. DAY, *Am. Chem. Soc. Symp. Ser.* **242** (1984) 424.
12. I. A. SERBINOV, G. A. NIKLASSON and C. G. GRANQVIST, *J. Mater. Sci. Lett.* **6** (1987) 1113.
13. W. WRASILDO, *J. Macromol. Sci.-Phys.* **B6** (1972) 559.
14. *Idem, J. Polym. Sci. Polym. Phys. Edn* **11** (1973) 2143.
15. E. SACHER, *IEEE Trans. Electr. Insul.* **EI-13** (1978) 94.
16. J. K. QUAMARA and B. L. SHARMA, *Acta Polym.* **36** (1985) 514.
17. E. SACHER, *J. Appl. Polym. Sci.* **22** (1978) 2137.
18. A. K. JONSCHER, *Phil. Mag. B* **38** (1978) 587.
19. L. A. DISSADO and R. M. HILL, *J.C.S., Faraday Trans. 2* **80** (1984) 291.
20. A. K. JONSCHER, "Dielectric Relaxation in Solids" (Chelsea Dielectrics Press, London 1983).
21. P. N. BUTCHER, *Phil. Mag. B* **37** (1978) 653.
22. P. N. BUTCHER and J. D. CLARK, *ibid.* **43**(1981) 1029.
23. G. F. LEAL FERREIRA, *Phys. Rev. B* **16** (1977) 4719.
24. H. SCHER and M. LAX, *ibid.* **7** (1973) 4491.
25. S. ALEXANDER, J. BERNASCONI, W. R. SCHNEIDER and R. ORBACH, *Rev. Mod. Phys.* **53** (1981) 175.
26. P. M. RICHARDS and R. L. RENKEN, *Phys. Rev. B* **21** (1980) 3740.
27. B. O'SHAUGHNESSY and I. PROCACCIA, *Phys. Rev. Lett.* **54** (1985) 455.
28. *Idem, Phys. Rev. A* **32** (1985) 3073.
29. J. R. BANAVAR and J. F. WILLEMSSEN, *Phys. Rev. B* **30** (1984) 6778.
30. R. A. GUYER, *Phys. Rev. A* **32** (1985) 2324.
31. S. ALEXANDER and R. ORBACH, *J. Phys. Lett.* **43** (1982) L625.
32. S. H. LIU, *Solid State Phys.* **39** (1986) 207.
33. M. F. SHLESINGER and B. D. HUGHES, *Physica* **109A** (1981) 597.

Received 30 April  
and accepted 22 October 1987